Stuart-type vortices on a rotating sphere

A. Constantin[1]†, and V. S. Krishnamurthy[2]

[1]Faculty of Mathematics, University of Vienna, Oskar-Morgenstern-Platz 1, 1090 Vienna, Austria

[2]Erwin Schrödinger International Institute for Mathematics and Physics, Boltzmanngasse 9, 1090 Vienna, Austria

(Received xx; revised xx; accepted xx)

Stuart vortices are among the few known smooth explicit solutions of the planar Euler equations with a nonlinear vorticity, and they have a counterpart for inviscid flow on the surface of a fixed sphere. By means of a perturbative approach we adapt the method used to investigate Stuart vortices on a fixed sphere to provide insight into some large-scale shallow water flows on a rotating sphere that model the dynamics of ocean gyres.

1. Introduction

Gyres are some of the most coherent features of the large-scale ocean circulation. There are five major gyres, centred around high pressure zones in the North Atlantic, North Pacific, South Atlantic, South Pacific, and the Indian Ocean, and a number of minor ones (for example, the Atlantic and the Pacific Ocean have three such gyres each and relatively small-scale gyres are encountered in the Mediterranean Sea). The gyres span hundreds to thousands of kilometres and these vast circular systems, made up of wind-driven ocean currents that spiral in slow-motion (with typical speed scale 0.1 $\mathrm{m\,s^{-1}}$) about a central point, rotate clockwise in the northern Hemisphere and counter-clockwise in the Southern Hemisphere due to the Coriolis effect. Their motion is typically not perfectly circular, with paths that can be more irregular and oval.

The Earth is nearly an oblate spheroid, with a small equatorial bulge as the polar radius is about 21 km shorter than the equatorial one (of length 6378 km), but in studies of large-scale ocean flows a spherical Earth model is adequate since no dynamical consequences of the small deviation from a perfect sphere have been observable in this regime (see *Wunsch* (2015)). Due to their large scales, the curvature of the Earth must be expected to play a significant rôle in the dynamics of gyre flows. Since the f-plane approximation does not capture curvature effects, most studies of ocean gyres are performed within the framework of the β-plane approximation (see *Talley et al.* (2011); *Vallis* (2006)), to the extent that the observed asymmetry of the gyres is known as the "β-effect", i.e., the change of the Coriolis parameter with latitude, which is ignored in the f-plane approximation (see *Cushman-Roisin and Beckers* (2011)). However, in contrast to the f-plane equations, the β-plane equations are not a consistent approximation to the governing equations for ocean flow in non-equatorial regions (see the discussions in *Dellar* (2011); *Paldor* (2015); *Stewart and Dellar* (2010)). Moreover, the vanishing of the meridional component of the Coriolis force at the Equator prevents the presence of gyres near the Equator, where the ocean flow is basically zonal (see the discussions in *Constantin* (2012); *Constantin and Johnson* (2015, 2016); *Henry* (2013, 2016)). These considerations motivate the study of ocean gyres in spherical geometry.

We investigate a class of solutions to the vorticity equation for shallow water flows on

† Email address for correspondence: adrian.constantin@univie.ac.at

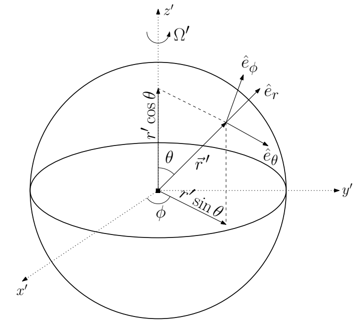

FIGURE 1. The Earth's rotating spherical coordinate system: θ is the polar angle, ϕ is the angle of longitude and $r' = |\vec{r'}|$ is the distance from the origin at the Earth's centre. The North Pole is at $\theta = 0$ and the Equator is on $\theta = \pi/2$.

a rotating sphere (derived recently in *Constantin and Johnson* (2017)) that correspond to the celebrated Stuart vortices in planar flows (see *Stuart* (1967)). By means of an interplay between results from the theory of elliptic partial differential equations and the geometric features encoded in the stereographic projection, we show that, for the relevant vorticity function, the counterpart of the Stuart vortices on a non-rotating sphere obtained in *Crowdy* (2004) represent the leading order of gyre-flow type solutions in a subregion of a rotating sphere, provided that the diameter of the gyre region is of the order of hundreds of km. This permits us to visualise the streamline-pattern of the flow on a rotating sphere. The viewpoint advocated in this paper is that in-depth studies of shallow-water flows on a rotating sphere can be pursued in spherical coordinates. These have the advantage with respect to the use of the β-plane approximation that they are capture the effects of the Earth's sphericity and are valid in any region of the sphere, whereas the β-plane equations are a consistent approximation only in equatorial regions.

2. Preliminaries

We introduce a set of (right-handed) spherical coordinates (r', θ, ϕ): r' is the distance from the centre of the sphere, θ (with $0 \leqslant \theta \leqslant \pi$) is the polar angle (and then $\pi/2 - \theta$ is the angle of latitude); ϕ (with $0 \leqslant \phi < 2\pi$) is the azimuthal angle i.e. the angle of longitude. We use primes, throughout the formulation of the problem, to denote physical (dimensional) variables; these will be removed when we non-dimensionalize. The unit vectors in this (r', θ, ϕ)-system are $(\hat{\mathbf{e}}_r, \hat{\mathbf{e}}_\theta, \hat{\mathbf{e}}_\phi)$, respectively, and the corresponding velocity components are (w', v', u'); $\hat{\mathbf{e}}_\phi$ points from West to East, and $\hat{\mathbf{e}}_\theta$ from North to South (see Fig. 1). The governing equations for inviscid flow are the Euler equation

$$\begin{aligned}
&\Big(\frac{\partial}{\partial t'} + \frac{u'}{r' \sin\theta}\frac{\partial}{\partial \phi} + \frac{v'}{r'}\frac{\partial}{\partial \theta} + w'\frac{\partial}{\partial r'}\Big)(w', v', u') \\
&\quad + \frac{1}{r'}\Big(- u'^2 - v'^2,\, -u'^2 \cot\theta + v'w',\, u'v' \cot\theta + u'w'\Big) \\
&\quad + 2\Omega' \left(-u' \sin\theta,\, -u' \cos\theta,\, v' \cos\theta + w' \sin\theta\right) - r' \Omega'^2 \left(\sin^2\theta,\, \sin\theta\cos\theta,\, 0\right) \\
&= -\frac{1}{\rho'}\Big(\frac{\partial p'}{\partial r'},\, \frac{1}{r'}\frac{\partial p'}{\partial \theta},\, \frac{1}{r' \sin\theta}\frac{\partial p'}{\partial \phi}\Big) + (-g', 0, 0)\,,
\end{aligned} \tag{2.1}$$

and the equation of mass conservation

$$\frac{1}{r'\sin\theta}\,\frac{\partial u'}{\partial\phi}+\frac{1}{r'\sin\theta}\,\frac{\partial}{\partial\theta}\,(v'\sin\theta)+\frac{1}{r'^2}\,\frac{\partial}{\partial r'}\,(r'^2\,w')=0\,, \tag{2.2}$$

respectively, where $p'(r',\theta,\phi,t')$ is the pressure in the fluid, $\Omega'\approx 7.29\times 10^{-5}$ rad s^{-1} is the constant rate of rotation of the Earth and ρ' is the constant density, with the choice $g'=$ constant ≈ 9.81 m s^{-2} for the gravitational term reasonable for the depths of the oceans on the Earth (see *Vallis* (2006)).

Redefining the pressure

$$p'=g'\rho'(R'-r')+\frac{1}{2}\rho' r'^2\Omega'^2\sin^2\theta+P'(r',\theta,\phi,t')\,, \tag{2.3}$$

where $R'\approx 6378$ km is the Earth's radius, and then writing

$$r'=R'+z'\,, \tag{2.4}$$

we non-dimensionalize the governing equations (2.1)-(2.2) for steady flow according to

$$z'=H'z\,,\qquad (w',\,v',\,u')=U'\,(kw,\,v,\,u)\,,\qquad P'=\rho' U'^2 P\,, \tag{2.5}$$

where H' is the mean depth of the ocean and U' is a suitable horizontal speed scale (typically of the order of 4 km and 0.1 m s^{-1}, respectively). The scaling factor, k, associated with the vertical component (w) of the velocity, is very small (of the order of 10^{-4}) since the vertical motion is so weak that it is almost always inferred rather than measured directly (see *Marshall and Plumb* (2016); *Viudez and Dritschel* (2015)). Defining the shallowness parameter ε by

$$\varepsilon=\frac{H'}{R'}\,, \tag{2.6}$$

the steady-state Euler equations become

$$\begin{aligned}&\Big(\frac{u}{(1+\varepsilon z)\sin\theta}\,\frac{\partial}{\partial\phi}+\frac{v}{1+\varepsilon z}\,\frac{\partial}{\partial\theta}+\frac{k}{\varepsilon}\,w\,\frac{\partial}{\partial z}\Big)(kw,\,v,\,u)\\&\quad+\frac{1}{1+\varepsilon z}\,\Big(-u^2-v^2,\,-u^2\cot\theta+kvw,\,uv\cot\theta+kuw\Big)\\&\quad+2\omega\,(-u\,\sin\theta,\,-u\cos\theta,\,v\cos\theta+kw\,\sin\theta)\\&=-\Big(\frac{1}{\varepsilon}\frac{\partial P}{\partial z},\,\frac{1}{1+\varepsilon z}\frac{\partial P}{\partial\theta},\,\frac{1}{(1+\varepsilon z)\sin\theta}\frac{\partial P}{\partial\phi}\Big)\,,\end{aligned} \tag{2.7}$$

where

$$\omega=\frac{\Omega' R'}{U'}\gg 1 \tag{2.8}$$

(with $\omega\approx 4650$ for $U'=0.1$ m s^{-1}), while the equation of mass conservation becomes

$$\frac{1}{(1+\varepsilon z)\sin\theta}\Big\{\frac{\partial u}{\partial\phi}+\frac{\partial}{\partial\theta}(v\sin\theta)\Big\}+\frac{k}{\varepsilon(1+\varepsilon z)^2}\,\frac{\partial}{\partial z}\Big\{(1+\varepsilon z)^2 w\Big\}=0\,. \tag{2.9}$$

Typically $k=\mathrm{O}(\varepsilon^2)$ (see the discussion in *Constantin and Johnson* (2017)) so that, multiplying the first component of (2.7) by ε and subsequently letting $\varepsilon\to 0$ (the shallow-water approximation), we see that the horizontal flow (u, v) is governed by the equations

$$0 = \frac{\partial P}{\partial z}\,, \tag{2.10}$$

$$\Big(\frac{u}{\sin\theta}\,\frac{\partial}{\partial\phi} + v\,\frac{\partial}{\partial\theta}\Big)v - u^2\cot\theta - 2\omega\,u\cos\theta = -\,\frac{\partial P}{\partial\theta}\,, \tag{2.11}$$

$$\Big(\frac{u}{\sin\theta}\,\frac{\partial}{\partial\phi} + v\,\frac{\partial}{\partial\theta}\Big)u + uv\cot\theta + 2\omega\,v\cos\theta = -\,\frac{1}{\sin\theta}\,\frac{\partial P}{\partial\phi}\,, \tag{2.12}$$

$$\frac{\partial u}{\partial\phi} + \frac{\partial}{\partial\theta}\,(v\sin\theta) = 0\,. \tag{2.13}$$

The existence of a stream function, $\psi(\theta, \phi)$, satisfying

$$u = -\frac{\partial\psi}{\partial\theta}\,, \qquad v = \frac{1}{\sin\theta}\,\frac{\partial\psi}{\partial\phi}\,, \tag{2.14}$$

is ensured by (2.13) and the elimination of the pressure between equations (2.11) and (2.12) gives the vorticity equation

$$\Big(\psi_\phi\,\frac{\partial}{\partial\theta} - \psi_\theta\,\frac{\partial}{\partial\phi}\Big)\Big(\frac{1}{\sin^2\theta}\,\psi_{\phi\phi} + \psi_\theta\cot\theta + \psi_{\theta\theta} - 2\omega\,\cos\theta\Big) = 0\,, \tag{2.15}$$

in which

$$\nabla^2_{\Sigma}\psi = \frac{1}{\sin^2\theta}\,\psi_{\phi\phi} + \psi_\theta\cot\theta + \psi_{\theta\theta}$$

is the Laplace-Beltrami expression. Writing equation (2.15) in the form

$$\psi_\phi(\nabla^2_{\Sigma}\psi - 2\omega\,\cos\theta)_\theta - \psi_\theta\,(\nabla^2_{\Sigma}\psi - 2\omega\,\cos\theta)_\phi = 0\,,$$

throughout regions where $\nabla_{(\phi,\theta)}\psi \neq (0, 0)$, the rank theorem (see *Newns* (1967)) yields

$$\nabla^2_{\Sigma}\psi - 2\omega\cos\theta = F(\psi) \tag{2.16}$$

for some function F. The total vorticity of the flow comprises two components: the vorticity solely due to the rotation of the Earth ($2\omega\,\cos\theta$: 'spin vorticity') and that due to the underlying motion of the ocean, $F(\psi)$, and not driven by the rotation of the Earth ('oceanic' or 'relative' vorticity). One of these contributions (the spin vorticity) is completely prescribed, but that associated with the movement of the ocean is specific to the particular flow conditions. Note that if we ignore the planetary (spin) vorticity by setting $\omega = 0$, equation (2.16) becomes the equation describing stationary vortex structures in an ideal fluid. The presence of planetary vorticity in equation (2.16) alters considerably the underlying mathematical structure of the problem due to the intricate coupling between the oceanic and the planetary vorticity components. For theoretical investigations of vortex dynamics in a bounded region of the surface of a non-rotating sphere we refer to *Crowdy* (2006); *Kidambi and Newton* (2000); *Newton* (2001).

Equation (2.16) is the counterpart in spherical coordinates of Fofonoff's β-plane model *Fofonoff* (1954), described in modern notation in *Vallis* (2006), and offers some exciting prospects for future investigations. For example, on the stereographically projected equatorial ξ-plane, equation (2.16) becomes

$$(1 + \xi\bar{\xi})^2\psi_{\xi\bar{\xi}} = 2\omega\,\frac{\xi\bar{\xi} - 1}{1 + \xi\bar{\xi}} + F(\psi)\,, \tag{2.17}$$

where $|\xi| = \cot(\frac{\theta}{2})$ for the polar angle $\theta \in (0, \pi)$; see Fig. 2. Explicit solutions for linear functions F were obtained in *Constantin and Johnson* (2017), e.g. for $F = \gamma$ (constant),

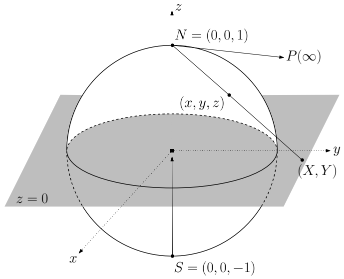

FIGURE 2. Schematic illustration of the stereographic projection mapping the point (x, y, z) on the unit sphere with the North Pole N excised to the intersection point (X, Y) of the equatorial plane with the ray from N to (x, y, z).

the general solution of (2.17) is given by

$$\psi(\xi,\bar{\xi}) = \gamma\ln(1+\xi\bar{\xi}) + \frac{2\omega}{1+\xi\bar{\xi}} + \zeta(\xi,\bar{\xi})\,, \tag{2.18}$$

where $\zeta(\xi,\bar{\xi})$ is an arbitrary harmonic function. The considerations related to Stuart vortices (see *Crowdy* (2004); *Stuart* (1967)) offer prospects for the study of the nonlinear vorticity function $F(\psi) = ae^{b\psi} + c$ with suitable real constants a, b, c.

3. Main result

We seek solutions of (2.17) for $F(\psi) = ae^{b\psi} + c$ with suitable real constants a, b, c. Setting

$$\psi(\xi,\bar{\xi}) = \zeta(\xi,\bar{\xi}) + A\ln(1+\xi\bar{\xi})\,, \tag{3.1}$$

for some real constant A to be determined, we get

$$\psi_{\xi\bar{\xi}} = \zeta_{\xi\bar{\xi}} + \frac{A}{(1+\xi\bar{\xi})^2}\,, \qquad e^{b\psi} = (1+\xi\bar{\xi})^{Ab}\,e^{b\zeta}\,,$$

and therefore (2.17) becomes

$$\zeta_{\xi\bar{\xi}} = \frac{c-A+2\omega}{(1+\xi\bar{\xi})^2} - \frac{4\omega}{(1+\xi\bar{\xi})^3} + ae^{b\zeta}\,(1+\xi\bar{\xi})^{Ab-2}\,.$$

For

$$A = \frac{2}{b}\,, \qquad c = A - 2\omega\,,$$

we see that (2.17) is transformed to the equation

$$\zeta_{\xi\bar{\xi}} = a\,e^{b\zeta} - \frac{4\omega}{(1+\xi\bar{\xi})^3}\,. \tag{3.2}$$

Setting $\omega = 0$ in (3.2) leads us to the Liouville equation

$$\zeta_{\xi\bar{\xi}} = a\,e^{b\zeta}\,, \tag{3.3}$$

which is exactly solvable. This feature enabled *Crowdy* (2004) to associate to any solution ζ_0 of (3.3) an explicit stream function

$$\psi_0(\xi,\bar{\xi}) = \zeta_0(\xi,\bar{\xi}) + \frac{2}{b}\,\ln(1+\xi\bar{\xi}) \tag{3.4}$$

that represents the flow pattern of Stuart-type vortices on a non-rotating sphere. We aim to show that for any gyre flow with nonlinear oceanic vorticity of the form

$$F(\psi) = a\, e^{b\psi} + \frac{2}{b} - 2\omega\,, \tag{3.5}$$

dependent on the inverse Rossby number $\omega \gg 1$ and on the free real parameters a, b with $ab > 0$, and such that the diameter d' of the gyre region satisfies

$$d' \sqrt{\frac{\Omega'}{U'R'}} = \mathrm{O}(1)\,, \tag{3.6}$$

the explicit functions in (3.4) are accurate approximations of the stream function ψ of the gyre flow, in the sense that

$$0 \leqslant \psi - \psi_0 \leqslant \frac{1}{4}\, \frac{\sin^6(\theta_S/2)}{\sin^2(\theta_N/2)}\, \frac{(d')^2\Omega'}{U'R'}\,, \tag{3.7}$$

where $\theta_N \in (0,\pi)$ and $\theta_S \in (0,\pi)$ are the co-latitudes of the northern, respectively southern tips, of the gyre region; here the diameter of a (not necessarily circular) planar or spherical region is defined as the largest distance between two points in the region. Intuitively, this result means that although the rotation term in (3.2) is large, its effect on the (highly nonlinear) dynamics can nevertheless be small if the size of the gyre region is relatively small, as quantified in (3.6) and (3.7). Physically realistic scenarios for the occurrence of such flows are provided in Section 5.

We rely on the theory of elliptic partial differential equations to prove the approximation property (3.7). Indeed, in terms of the Cartesian coordinates (X, Y) in the complex ξ-plane, we can write (3.2) as the semilinear elliptic equation

$$\Delta\zeta = 4a\, e^{b\zeta} - \frac{16\omega}{(1+X^2+Y^2)^3}\,, \tag{3.8}$$

where $\Delta = \partial_X^2 + \partial_Y^2$ is the Laplace operator, while (3.3) becomes

$$\Delta\zeta = 4a\, e^{b\zeta}\,. \tag{3.9}$$

At the ocean surface, a gyre is delimited by a level set of the stream function, say $\psi = 0$, which encloses a region $\mathcal{O}'$ on the surface of the sphere and this spherical region corresponds in the (X, Y)-coordinates to a planar region $\mathcal{O}$, the scaled stereographic projection of $\mathcal{O}'$. Consequently we have to solve for

$$\gamma = \zeta - \zeta_0$$

the equation

$$-\Delta\gamma + 4a\, e^{b\zeta_0}(e^{b\gamma} - 1) - \frac{16\omega}{(1+X^2+Y^2)^3} = 0 \tag{3.10}$$

in a bounded planar domain $\mathcal{O}$, with homogeneous Dirichlet boundary data

$$\gamma = 0 \quad \text{on} \quad \partial\mathcal{O}\,, \tag{3.11}$$

where $\partial\mathcal{O}$ is the smooth boundary of $\mathcal{O}$. In our analysis we apply the method of sub- and super-solutions, combined with maximum principles and elliptic *a priori* estimates.

We recall that the classical Calderón-Zygmund theory for the linear Dirichlet problem

$$\begin{cases} \Delta U_0 = F_0 \quad \text{in} \quad \mathcal{O}\,, \\ U_0 = 0 \quad \text{on} \quad \partial\mathcal{O}\,, \end{cases} \tag{3.12}$$

in the setting of Sobolev spaces, asserts that if $F_0 \in L^2(\mathcal{O})$, then there exists a unique solution $U_0 \in H^2(\mathcal{O}) \cap H_0^1(\mathcal{O})$ of (3.12) and the following estimate holds:

$$\|U_0\|_{H^2(\mathcal{O})} \leqslant C_0 \|F_0\|_{L^2(\mathcal{O})} \tag{3.13}$$

for some constant $C_0 > 0$ depending only on $\mathcal{O}$; see *Brézis* (2011) and *Ponce* (2016). Moreover, if F_0 is the restriction of a continuous function $F_0 : \mathbb{R}^2 \to \mathbb{R}$ to $\mathcal{O}$, then U_0 is twice continuously differentiable in $\mathcal{O}$ and admits a continuous extension to the closure $\overline{\mathcal{O}} = \mathcal{O} \cup \partial\mathcal{O}$ of $\mathcal{O}$; see *Gilbarg and Trudinger* (2001). Note that in terms of the Green's function of the first kind for $\mathcal{O}$, $G_{\mathcal{O}}(X, Y, X', Y')$, we have

$$U_0(X,Y) = \iint_{\mathcal{O}} G_{\mathcal{O}}(X,Y,X',Y')\, F_0(X',Y')\, dX'dY' \,, \qquad (X,Y) \in \mathcal{O} \,. \tag{3.14}$$

In particular, for circular domains the Green's function $G_{\mathcal{O}}(X, Y, X', Y')$ is explicitly determined (see *Gilbarg and Trudinger* (2001)). Also, for annular domains an explicit Green's function is available (see *Crowdy and Marshall* (2007)). While the estimate (3.13) and the representation formula (3.14) are important for the existence of solutions, we will take advantage of the following growth estimate for the solution of (3.12):

$$0 \leqslant U_0(X,Y) \leqslant \frac{1}{16}\, M D^2 \,, \qquad (X,Y) \in \mathcal{O} \,, \tag{3.15}$$

where D is the diameter of the set $\mathcal{O}$ and

$$0 \leqslant M = \max_{(X,Y)\in\overline{\mathcal{O}}} \{-F_0(X,Y)\} \quad \text{for} \quad F_0 : \overline{\mathcal{O}} \to (-\infty, 0] \quad \text{continuous}\,.$$

To prove (3.15), note that since $F_0 \leqslant 0$, the weak maximum principle (see *Gilbarg and Trudinger* (2001)) ensures that the minimum of the solution U_0 in $\overline{\mathcal{O}}$ is attained on the boundary $\partial\mathcal{O}$, and thus $U_0 \geqslant 0$ throughout $\overline{\mathcal{O}}$. Furthermore, if $(X_0, Y_0) \in \overline{\mathcal{O}}$ is a point such that $\overline{\mathcal{O}}$ is contained within the closed ball of radius $D/2$ centred at this point, then the function $\tilde{U}$ defined by

$$\tilde{U}(X,Y) = U_0(X,Y) + \frac{M[4(X-X_0)^2 + 4(Y-Y_0)^2 - D^2]}{16} \,, \qquad (X,Y) \in \overline{\mathcal{O}} \,,$$

is such that $\Delta\tilde{U} \geqslant 0$ in $\mathcal{O}$ and $\tilde{U} \leqslant 0$ on $\partial\mathcal{O}$. The weak maximum principle therefore ensures that the maximum of the solution $\tilde{U}$ in $\overline{\mathcal{O}}$ is attained on the boundary $\partial\mathcal{O}$, so that $\tilde{U} \leqslant 0$ throughout $\overline{\mathcal{O}}$ and this proves the upper estimate in (3.15).

On the other hand, twice continuously differentiable functions $\gamma_*\,, \gamma^* : \mathcal{O} \to \mathbb{R}$ with continuous extensions to $\overline{\mathcal{O}}$ which vanish on the boundary $\partial\mathcal{O}$, are called a *sub-solution* (*super-solution*) of (3.10) with the homogeneous Dirichlet boundary condition (3.11) if

$$-\Delta\gamma_* + 4ae^{b\zeta_0}\,(e^{b\gamma_*} - 1) - \frac{16\omega}{(1+X^2+Y^2)^3} \leqslant 0 \,, \qquad (X,Y) \in \mathcal{O} \,, \tag{3.16}$$

respectively if

$$-\Delta\gamma^* + 4ae^{b\zeta_0}\,(e^{b\gamma^*} - 1) - \frac{16\omega}{(1+X^2+Y^2)^3} \geqslant 0 \,, \qquad (X,Y) \in \mathcal{O} \,. \tag{3.17}$$

Since the nonlinearity in (3.10) is smooth, the method of sub- and super-solutions applies: the existence of a sub-solution γ_* and of a super-solution γ^* with $\gamma_* \leqslant \gamma^*$ in $\mathcal{O}$ ensures the existence of a solution γ that is twice continuously differentiable in $\mathcal{O}$, admits a continuous extension to $\overline{\mathcal{O}}$ and satisfies $\gamma_* \leqslant \gamma \leqslant \gamma^*$ throughout $\overline{\mathcal{O}}$; see *Ponce* (2016).

Let now ζ_0 be a solution of the Liouville equation (3.9), in a domain $\mathcal{O}$ delimited by a zero level set of ψ_0 defined by (3.4), and let U_0 be the unique solution of (3.12) with the homogeneous Dirichlet boundary condition $U_0 = 0$ on $\partial\mathcal{O}$, for

$$F_0(X,Y) = -\frac{16\omega}{(1+X^2+Y^2)^3}\,. \tag{3.18}$$

We now claim that $\gamma_* = 0$ is a sub-solution and $\gamma^* = U_0$ is a super-solution of (3.10), with $\gamma_* \leqslant \gamma^*$ in $\mathcal{O}$. Indeed, since $F_0 < 0$, the strong maximum principle (see *Gilbarg and Trudinger* (2001)) yields

$$U_0(X,Y) > 0\,, \qquad (X,Y) \in \mathcal{O}\,, \tag{3.19}$$

so that $\zeta_* < \zeta^*$ in $\mathcal{O}$ and

$$ae^{b(\zeta_0+U_0)} \geqslant ae^{b\zeta_0} \quad \text{in} \quad \mathcal{O} \quad \text{since} \quad ab > 0\,,$$

with the inequalities (3.16)-(3.17) now easily checked. The method of sub- and super-solutions therefore ensures the existence of a solution γ to (3.10) with homogeneous Dirichlet boundary data (3.11), such that

$$0 \leqslant \gamma \leqslant U_0 \quad \text{in} \quad \mathcal{O}\,. \tag{3.20}$$

Using (3.1), (3.4) and (3.15), we get

$$0 \leqslant \psi - \psi_0 = \gamma \leqslant U_0 \leqslant \frac{1}{16}\,MD^2 \quad \text{throughout} \quad \mathcal{O}'\,. \tag{3.21}$$

Since

$$1 + X^2 + Y^2 = 1 + |\xi|^2 = \frac{1}{\sin^2(\frac{\theta}{2})}\,,$$

we see that (3.18) in combination with (3.21) yield

$$0 \leqslant \psi - \psi_0 \leqslant \omega D^2 \sin^6\left(\frac{\theta_S}{2}\right) \quad \text{throughout} \quad \mathcal{O}'\,, \tag{3.22}$$

where θ_S is the co-latitude of the southern tip of the gyre region $\mathcal{O}'$ and D is the diameter of the (scaled) planar stereographic projection $\mathcal{O}$ of the spherical region $\mathcal{O}'$. Note that the stereographic projection distorts areas, with the infinitesimal distortion rate from the sphere to the plane equal to $4\sin^2(\frac{\theta}{2})$; in particular, planar projections of spherical areas near the South Pole are diminished while the projections of spherical areas near the North Pole are inflated. Therefore the diameter d' of the gyre region $\mathcal{O}'$ satisfies

$$\frac{d'}{R'} \geqslant 2D\,\sin\left(\frac{\theta_N}{2}\right),$$

where θ_N is the co-latitude of the northern tip of $\mathcal{O}'$. Using the above inequality in (3.22) validates the estimate (3.7), due to (2.8).

Since $\gamma = \psi - \psi_0 = \zeta - \zeta_0$ vanishes on $\partial\mathcal{O}$, with ζ_0 and ψ_0 both known explicitly within $\mathcal{O}$, to appreciate the relevance of the estimate (3.7) for revealing the streamline pattern of the flow, let us show that the range of (real) values of ζ_0 throughout $\mathcal{O}$ can be very wide for suitable choices of the free parameters a and b. To prove this, let us assume without loss of generality that $a > 0$, and so $b > 0$. Firstly, since $\psi_0 = 0$ on $\partial\mathcal{O}$, from (3.4) we infer that

$$\zeta_0 = -\frac{2}{b}\,\ln(1+\xi\bar{\xi}) \leqslant 0 \quad \text{on} \quad \partial\mathcal{O}\,. \tag{3.23}$$

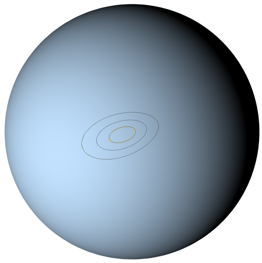

FIGURE 3. Depiction of the streamline pattern on the rotating sphere for the choice $f(z) = z^2+1$ and $a = 1$, $b\omega^2 = 2$ in (4.1).

We now prove that if $m > 0$ is such that

$$\frac{4me^{bm}}{a} \leqslant d_0^2 \,. \tag{3.24}$$

where d_0 is the diameter of the largest ball contained within the planar region $\mathcal{O}$, then

$$\inf_{(X,Y)\in\mathcal{O}} \{\zeta_0(X,Y)\} < -m \,. \tag{3.25}$$

To verify the estimate (3.25), let us first note that since $\zeta_0 \leqslant 0$ on $\partial\mathcal{O}$ and $\Delta\zeta_0 > 0$ in $\mathcal{O}$ is ensured by the fact that ζ_0 solves (3.9), the weak maximum principle yields $\zeta_0 < 0$ throughout $\mathcal{O}$. If $\mathcal{B}_0$ is the largest ball contained within the planar region $\mathcal{O}$ that is bounded by the smooth streamline $\psi_0 = 0$, then the circle $\partial\mathcal{B}_0$ that surrounds $\mathcal{B}_0$ will be tangent to $\partial\mathcal{O}$. Define the function

$$\alpha_0(X,Y) = \zeta_0(X,Y) - \frac{ae^{-bm}\,[4(X-X^0)^2 + 4(Y-Y^0)^2 - d_0^2]}{4}\,, \qquad (X,Y) \in \mathcal{B}_0\,,$$

where (X^0, Y^0) is the centre of the disk $\mathcal{B}_0$. Assuming that (3.25) is invalid, we would get $\zeta_0 \geqslant -m$ throughout $\mathcal{O}$, and (3.9) would yield $\Delta\zeta_0 \geqslant 4ae^{-bm}$ in $\mathcal{B}_0 \subset \mathcal{O}$. But then, since $\alpha_0 \leqslant 0$ on $\partial\mathcal{B}_0$ and $\Delta\alpha_0 = \Delta\zeta_0 - 4ae^{-bm} \geqslant 0$ in $\mathcal{B}_0$, the weak maximum principle would ensure that $\alpha_0 < 0$ throughout $\mathcal{B}_0$. In particular, $\alpha_0(X^0,Y^0) < 0$, that is,

$$\zeta_0(X^0,Y^0) < -\frac{ae^{-bm}}{4}\, d_0^2 \,.$$

But (3.24) then leads us to $\zeta_0(X^0,Y^0) < -m$, which is in contradiction with the assumption of the invalidity of (3.25). Consequently (3.25) must hold.

The estimates (3.7), (3.23) and (3.25) show that if the diameter of the gyre region satisfies (3.6), then the streamline pattern for ψ is a small perturbation of the level sets of the explicit function ψ_0.

4. Flow visualization

The form of the general solution to the Liouville equation (3.3) is (see *Henrici* (1986))

$$\zeta(z,\bar{z}) = \frac{1}{b\omega^2}\,\log\Big(\frac{4|f'(z)|^2}{(2 - ab\omega^2|f(z)|^2)^2}\Big)\,, \tag{4.1}$$

where f is a meromorphic function with $f' \neq 0$, $|f| \neq \frac{\sqrt{2}}{\omega\sqrt{ab}}$, and having at most isolated simple pole singularities in the domain in which the equation is to be solved. By means of (3.1) and (4.1), we can visualize the streamlines for various choices of

f (see Fig. 3 for an example that captures the flow pattern of a large gyre). For a given f, any closed streamline can be used to define the boundary of the relevant flow region. Note that typical gyre regions on the surface of the sphere are mapped by the stereographic projection into simply connected regions of the complex plane, for which the representation of the Green's function (corresponding to the Laplace operator) by the Riemann mapping function is classical (see *Henrici* (1986)). Moreover, we can approximate the boundary of a region of specific geophysical interest by a polygonal line with a high degree of accuracy, in which case the Schwarz-Christoffel formulas provide an explicit representation for the Riemann mapping function (see *Henrici* (1986)). In this context, we point out that if $\mathcal{O}$ is a simply connected bounded region of the complex plane, and $\mathfrak{g}(z,z') = -\log|z-z'| - \mathfrak{h}(z,z')$ is its Green's function for the Laplace operator, then $\zeta(\xi) = \mathfrak{h}(\xi,\xi)$ solves Liouville's equation $\Delta\zeta = 4e^{2\zeta}$ (see *Gustafsson* (1990)).

5. Discussion

Let us now comment on the physical relevance of the above theoretical considerations. For the reference value $U' = 0.1$ m s^{-1}, due to (3.6), gyre regions with a diameter of the order of 100 km enter our framework. One such example is the small-scale but energetic Ierapetra gyre, showing up in the Eastern Mediterranean, South-East of Crete, at the end of summer almost every year (see *Amitai et al.* (2010)); in this case $\theta_N \approx 55.5°$ and $\theta_S \approx 56.5°$, so that the upper bound in (3.7) is about 0.01. Gyre regions of a similar size occur in the Bering Sea (see the discussion in *Kostianov et al.* (2004)); in this case $\theta_N \approx 29.5°$ and $\theta_S \approx 30.5°$, so that the upper bound in (3.7) is about 0.001. Also, one of the most prominent features of the Arctic Ocean is the large Beaufort Gyre – a clockwise ocean current that, due to the interplay between the forces of gravity and Coriolis, circulates with its overlying sea ice cover with surface speeds of the order 0.1 m s^{-1} in the region comprised between 76°N-84°N and 140°W-180°E; see the data in *Plueddemann et al.* (2017). The corresponding polar angle θ for the Beaufort Gyre is between 6° and 14°, and in this case the upper bound in (3.7) is less than 0.05, despite the relatively large gyre diameter – a feature that is offset by the co-latitude factor.

Concerning gyre flows in the Southern Hemisphere, consider the clockwise oceanic gyres in the Weddell and Ross Sea: with surface current speeds of the order of 0.1 m s^{-1}, diameters of about 2000 km, and corresponding values $\theta_N \approx 150°$ and $\theta_S \approx 160°$ (see *Riffenburgh* (2007)), these gyres dominate the ocean circulation in each basin, being confined between the continent of Antarctica and the azimuthal flow of the Antarctic Circumpolar Current – the most significant current in our oceans and the only current that completely encircles the polar axis, being composed of a number of high-speed, vertically coherent, seafloor-reaching jets with speeds commonly exceeding 1 m s^{-1} and typically 40-50 km wide, separated by zones of low-speed flow (see the discussion in *Constantin and Johnson* (2016)). In this case the upper bound in (3.7) is about 100, and thus of no practical relevance. However, rather than performing the stereographic projection from the North Pole, in this case we can rely on that from the South Pole, with the outcome that (3.7) holds with θ replaced by $\pi - \theta$, resulting in an upper bound less than 2. While this may be still relevant, the obtained value shows that the diameter of these gyres is too large to be amenable to the approach pursued in this paper. This will also be the case for the largest oceanic gyres (e.g. in the North Pacific and Southern Atlantic). Nevertheless, our considerations are physically relevant for the dynamics of small- and mid-size gyres (with diameters of the order of several hundreds km).

Acknowledgements This research was supported by the WWTF research grant MA16-009

(A.C.) and by the ESI Junior Research Fellowship Programme (V.S.K.). The authors are grateful for the suggestions and comments made by the referees.

REFERENCES

Amitai, Y., and Lehahn, Y., and Lazar, A., and E. Heifetz (2010), Surface circulation of the eastern Mediterranean Levantine basin: Insights from analyzing 14 years of satellite altimetry data, *J. Geophys. Res.*, *115*, C10058.

Brézis, H. (2011), *Functional analysis, Sobolev spaces and partial differential equations*, Universitext, Springer, New York.

Constantin, A. (2012), An exact solution for equatorially trapped waves, *J. Geophys. Res.: Oceans*, *117*, Art. C05029.

Constantin, A., and R. S. Johnson (2015), The dynamics of waves interacting with the Equatorial Undercurrent, *Geophys. Astrophys. Fluid Dyn.*, *109*, 311–358.

Constantin, A., and R. S. Johnson (2016), An exact, steady, purely azimuthal equatorial flow with a free surface, *J. Phys. Oceanogr.*, *46*, 1935–1945.

Constantin, A., and R. S. Johnson (2016), An exact, steady, purely azimuthal flow as a model for the Antarctic Circumpolar Current, *J. Phys. Oceanogr.*, *46*, 3585–3594.

Constantin, A., and R. S. Johnson (2017), Large gyres as a shallow-water asymptotic solution of Euler's equation in spherical coordinates, *Proc. Roy. Soc. A*, *473*, Art. 20170063.

Crowdy, D. G. (1997), General solutions to the 2D Liouville equation, *Intl J. Engng. Sci*, *35*, 141–149.

Crowdy, D. G. (2004), Stuart vortices on a sphere, *J. Fluid Mech.*, *398*, 381–402.

Crowdy, D. G. (2006), Point vortex motion on the surface of a sphere with impenetrable boundaries, *Phys. Fluids*, *18*, Art. 036602.

Crowdy, D. G., and J. Marshall (2007), Green's functions for Laplace's equation in multiply connected domains, *IMA J. Appl. Math.*, *72*, 278–301.

Cushman-Roisin, B., and J.-M. Beckers (2011), *Introduction to geophysical fluid dynamics: physical and numerical aspects*, Academic Press, New York.

Dellar, P. J. (2011), Variations on a beta-plane: derivation of non-traditional beta-plane equations from Hamilton's principle on a sphere, *J. Fluid Mech.*, *674*, 174–195.

Fofonoff, N. P. (1954), Steady flow in a frictionless homogeneous ocean, *J. Mar. Res.*, *13*, 254–262.

Gilbarg, D., and N. S. Trudinger (2001), *Elliptic partial differential equations of second order*, Springer-Verlag, Berlin.

Gustafsson, B. (1990), On the convexity of a solution of Liouville's equation, *Duke Math. J.*, *60*, 303–311.

Henrici, P. (1986), *Applied and computational complex analysis*, Vol. 3, John Wiley & Sons, Inc., New York, 1986.

Henry, D. (2013), An exact solution for equatorial geophysical water waves with an underlying current, *Eur. J. Mech. B (Fluids)*, *38*, 18–21.

Henry, D. (2016), Equatorially trapped nonlinear water waves in a β-plane approximation with centripetal forces, *J. Fluid Mech.*, *804*, R1, 11 p.

Kidambi, R., and P. Newton (2000), Point vortex motion on a sphere with solid boundaries, *Phys. Fluids*, *12*, 581–588.

Kostianov, A. G., and Nihoul, J. C. J., and V. B. Rodionov (2004), *Physical oceanography of frontal zones in the subarctic seas*, Elsevier.

Marshall, J., and R. A. Plumb (2016), *Atmosphere, ocean and climate dynamics: an introductory text*, Academic Press, London.

Newns, W. F. (1967), Functional dependence, *Amer. Math. Monthly*, *74*, 911–920.

Newton, P. K. (2001), *The N-vortex problem*, Springer-Verlag.

Paldor, N. (2015), *Shallow water waves on the rotating Earth*, Springer, Cham.

Plueddemann, A. J., and Krishfield, R., and Takizawa, T., and Hatakeyama, K., and S. Honjo (1998), Upper ocean velocities in the Beaufort Gyre, *Geophys. Res. Lett.*, *25*, 183–186.

Ponce, A. C. (2014), *Elliptic PDEs, measures and capacities. From the Poisson equations* *to nonlinear Thomas-Fermi problems*, EMS Tracts in Mathematics, 23, European Mathematical Society (EMS), Zürich.

Riffenburgh, B. (2007), *Encyclopedia of the Antarctic*, Routledge.

Stewart, A. L., and P. J. Dellar (2010), Multilayer shallow water equations with complete Coriolis force. Part 1. Derivation on a non-traditional beta-plane, *J. Fluid Mech.*, *651*, 387–413.

Stuart, J. T. (1967), On finite amplitude oscillations in laminar mixing layers, *J. Fluid Mech.*, *29*, 417–440.

Talley, L. D., and Pickard, G. L., and Emery, W. J., and J. H. Swift (2011), *Descriptive physical oceanography: an introduction*, Elsevier, London.

Vallis, G. K. (2006), *Atmosphere and ocean fluid dynamics*, Cambridge University Press, Cambridge.

Viudez, A., and D. G. Dritschel (2015), Vertical velocity in mesoscale geophysical flows, *J. Fluid Mech.*, *483*, 199–223.

Wunsch, C. (2015), *Modern observational physical oceanography*, Princeton University Press, Princeton, 2015.